Desalination and Water Treatment
www.deswater.com

doi: 10.5004/dwt.2023.29859

307 (2023) 72–81
September

The uptake efficiency of phosphate ions using Jordanian calcinated bentonite

Hutaf M. Baker[a,*], Mousa Al-Mutairy[a], Hamzeh M. Abdel-Halim[b]

[a]*Department of Chemistry, Faculty of Science, Al al-Bayt University, P.O. Box: 130091, Mafraq 25113, Jordan, emails: hutafb@aabu.edu.jo/hutafb@yahoo.com (H.M. Baker), chemchem112@live.com (M. Al-Mutairy)*
[b]*Department of Chemistry, The Hashemite University, Zarqa 13133, Jordan, email: hamzehah@hu.edu.jo*

Received 6 May 2023; Accepted 11 August 2023

ABSTRACT

The investigation of the adsorption potential of the Jordanian calcinated bentonite to remove phosphate ions from aqueous solutions whether they are synthetic or actual samples was studied in this article, The temperatures for calcination ranged from (100°C–900°C). The effectiveness of calcining bentonite's ability to remove phosphate ions was investigated under various conditions, including initial concentration of phosphate ions, calcinations, temperature, particle size, pH levels, adsorbent dose, and contact time. Using pseudo-first-order, pseudo-second-order rates and intraparticle diffusion models the kinetic studies were carried out. The R^2 values indicated that pseudo-second-order rather than pseudo-first-order provided a better fit for the phosphate transport. The activation energy for the removal for both synthetic and actual materials was computed, and it was found to be 8.93 and 12.120 kJ/mol, respectively, this shows that physisorption may have happened. The rate of phosphate ion uptake was also investigated using intraparticle diffusion model at different variables (temperature, particle size, agitation, and pH values), and both particle diffusion (D_p) and film diffusion (D_f) coefficients were predicted, with the results indicating that film diffusion (D_f) is the rate determining step.

Keywords: Bentonite; Calcinated, Removal; Kinetics; Wastewater

1. Introduction

For economic growth, human existence, and the health of ecosystems, water is a crucial resource. The demand for water has, however, increased significantly due to exponential population growth, rapid industrialization, urbanization, and agricultural expansion, which has led to the production of large volumes of wastewater with a higher concentration of various pollutants, including phosphate that has a negative impact on the environment and ecosystems [1]. This inorganic oxyanions (phosphate ion) is harmful to humans and wildlife at certain concentrations. When phosphate levels in water exceed 0.02 mg/L, eutrophication of freshwater lakes, reservoirs, streams, and headwaters of estuarine systems occurs, this decrease in dissolved oxygen in the aqueous environment kills aquatic life and upsets the natural food chain, among other effects. The degradation of water's fitness for human use caused by phosphate contamination of surface waters also has an impact on marine life [2,3].

Phosphate removal from wastewater is difficult, necessitating innovation in treatment technology development. Phosphate removal procedures are classified as physical, chemical, or biological. Physical traditional wastewater treatment technologies have a relatively poor phosphate removal effectiveness (5%–10%). Electrodialysis and reverse osmosis, for example, are extremely expensive. Because most phosphorus compounds in wastewater are water-soluble chemical precipitation has become the most used approach for removing phosphate from wastewater. However, chemical treatment methods are not acceptable due to high operational costs for chemicals and an increase in chemical sludge volume of up to 40% that is difficult to

* Corresponding author.

dispose of, and effluent neutralization has a number of problems, precipitation using chemical treatment removes only a small fraction. Enhanced biological phosphorus elimination is becoming a regular way of biological treatment. However, the technique is prone to unpredictability due to the unsuccessful or reduced activity of polyphosphate-accumulating organisms, such as free nitrous acid synthesis, which inhibits biological processes. Advanced biological methods can remove up to 97% of phosphate and generate low amounts of sludge but the method has limited practical applicability [4–7]. As a result, developing new and low-cost remediation solutions to reduce pollution and enhance surface water quality has become critical. Adsorption onto low-cost and readily accessible materials in wastewater treatment has lately sparked considerable attention due to its efficacy. The studies of phosphorus immobilization by adsorption have been attracting more and more research interest in recent years for the saving of phosphate resources and the recycling of phosphate. Some researchers focus on activated alumina, iron-based compounds, and polymeric ligand exchanger while others put more attention on natural materials and their modifications, such as clay like bentonite, kaolinite and zeolite which are used to treat cationic and anionic pollutants, [8–10]. Bentonite is any clay of volcanic origin that contains montmorillonite. It is made up of two silicon-oxygen tetrahedral sheets and one aluminium-oxygen-hydroxyl octahedral sheet in a 2:1 configuration.

Jordanian bentonite from Al Azraq (JBA) was used as an adsorbent in this investigation since it is a common clay element of soils and aquifers, The selected sorbent should be easy to handle, locally available adsorbents, has the efficiency in removing contaminants and inexpensive for that Jordanian bentonite was chosen.

The JBA was modified utilizing the calcination process to improve solid–liquid extraction with regard to phosphate.

According to our knowledge, this is the first study that using calcinated bentonite (JBA) to evaluate the elimination of the phosphate ion from aqueous solutions under different variables such as contact time, pH, initial concentration of phosphate ion, etc. The kinetic models were investigated also to understand the mechanism of phosphate removal.

1.1. Adsorption kinetics

Adsorption data was studied using pseudo-first-order, pseudo-second-order, and intraparticle diffusion models to better understand the process's kinetics.

1.1.1. Pseudo-first-order kinetic model

The linearized form of pseudo-first-order model (Lagergren) equation can be written as follows:

$$\log\left(q_e - q_t\right) = \log q_e - \frac{k_1 t}{2.303} \tag{1}$$

where q_e and q_t are the amount of phosphate exchanged (mg/g) at equilibrium and at time 't', respectively. k_1 (min^{-1}) is the rate constant of pseudo-first-order reaction. A plot of $\log(q_e - q_t)$ vs. t is expected to yield a straight line and the rate constant k_1 can be evaluated from the slope.

1.1.2. Pseudo-second-order model

The data may be fitted to the pseudo-second-order kinetic model which can be expressed as:

$$\frac{t}{q_t} = \frac{1}{k_2 q_e^2} + \frac{1}{q_e} t \tag{2}$$

where the boundary conditions of $t = 0$ to $t = t$ and $q_t = 0$ to $q_t = q_t$ has been considered. Here, k_2 is the rate constant for pseudo-second-order reaction (g/mg·min). The notation q_e and q_t denotes the amounts of solute removed at equilibrium and at any time 't' (mg/g), respectively. A plot of t/q_t vs. t is expected to yield a straight line and the values of q_e and k_2 can be determined from the slope and intercept, respectively [8,11–12].

1.1.3. Ion exchange modeling

The particle and film diffusion models were utilized to estimate the rate-controlling phase of the process in order to assess the diffusion coefficient. Given particle diffusion control and infinite volume boundary constraints, Vermeulen's model for the fractional attainment equilibrium, $U(t)$, is expressed as:

$$U\left(t\right) = \left[-1\exp\left(\frac{-D_p \pi^2 t}{r_p^2}\right)^{\frac{1}{2}}\right] \tag{3}$$

where $U(t)$ is defined as ratio between phosphate mass removed at the certain time and the maximum phosphate removed, D_p is the intraparticle diffusion coefficient in the ion expressed in m^2/s and r_p is the radius of the particle (m).

The film diffusion control model with infinite boundary conditions is described by the following equation:

$$U\left(t\right) = 1 - \exp\left(\frac{-3 D_f C t}{r_p \delta C^*}\right) \tag{4}$$

where D_f is the diffusion coefficient in the film (m^2/s), C and C^* is the phosphate concentrations in the solution and in the ion exchanger, respectively (mol/L), δ is the film thickness accepted as 10^{-4} cm for poorly stirred solution.

The linearization of Eqs. (3) and (4) give Eqs. (5) and (6):

$$-\ln\left(1 - U\left(t\right)^2\right) = t\left(\frac{D_p \pi^2}{r_p^2}\right) \tag{5}$$

$$-\ln\left(1 - U\left(t\right)\right) = t\left(3\frac{D_f C}{r_p \delta C^*}\right) \tag{6}$$

To find D_p and D_f, respectively, $-\ln(1-U(t)^2)$ and $-\ln(1-U(t))$ will be plotting against the time t [8,11–12].

2. Experimental setup

2.1. Chemicals and reagents

$NaH_2PO_4·H_2O$ (98% Gainland Chemical Company), NaOH (98% Desdide. Clwyd, UK), HCl (35.4%–36% Gainland Chemical Company), $(NH_4)_6MO_7O_{24}·4H_2O$ (98% DHD GPR), $C_6H_8O_6$ (99% Aldrich Chemistry), $C_8H_4K_2O_{12}Sb_2·3H_2O$ (≥98% Aldrich Chemistry), $C_{16}H_{18}N_3SCl$ (99% BDH Limited Pool, England), H_2SO_4 (98% Central Drug House), $AgNO_3$ (S.D. Fine Chem. Ltd), $(C_{16}H_{33})N^+(CH_3)_3Br^-$ (98% S.D. Fine Chem. Ltd).

2.1.1. Instruments and apparatus

UV/Vis Spectrometer (UNICAM900). Sieves and sieves machine, Analytical balance (METTLE$R TOLEDO, AL104), Digital pH meter (METTLE$R TOLEDO, Seven Easy), Centrifuge (CN180, Turkey), Muffle Furnace (SELECTHORN, Spain), Water bath shaker (GFL 10983), Heating Draying Oven (Model DHG), Hotplate stirrer (Labtech). Mechanical stirrer, three plates (Wisetire HS-30D).

2.1.2. Adsorbent preparation

Bentonite (JBA) was mined at Al Azraq (natural resources authority). Bentonite was cleaned to remove fines and other undesired material by soaking clays in deionized water for 24 h with moderate agitation on a regular basis. The material was washed many times to guarantee full elimination of all charge ions, then dried overnight at 97°C before being crushed. This (JBA) was then calcined in a muffle furnace for 4 h at various temperature values ranging from 100°C to 900°C in order to increase its mechanical resistance and to eliminate some impurities [13]. before being stored in tight screw bottles. The calcinated samples (CJBA) were categorized into particle sizes ranging from 38 to 125 m on average.

2.1.3. Physical characteristics of adsorbent

The bulk density, porosity, specific surface area, and cation exchange capacity (CEC) of (JBA) and (CJBA) were calculated [14], and the findings are reported in Table 1.

The mineralogical compositions of this bentonite were investigated using X-ray diffraction (XRD), scanning electron micrograph (SEM), and X-ray fluorescence (XRF), as shown in Tables 2 and 3 and Figs. 1 and 2.

2.1.4. Real wastewater sample

The king Talal dam provided real wastewater. It was treated with 1 mL/1 L H_2SO_4 to guarantee that no alterations occurred until the research was completed.

2.2. Batch adsorption experiments

Many variables were investigated like contact time, particle size, temperature of calcinations, initial phosphate concentration, temperature, pH, and adsorbent dose using calcinated bentonite to get the optimal conditions for the removal of phosphate ions from aqueous media, the batch method was applied. All the samples measured using UV/Vis Spectrometer (UNICAM900) at λ = 875 nm after centrifugation. All the chemical reagents that used are analytical grade. 25 mL of synthetic phosphate solution with 1.0000 g of adsorbent were used in each variable.

The calcination was carried out using samples of bentonite clay in range of 100°C–900°C. The other conditions were maintained constant (i.e., temperature at 25°C temperature, pH equal 8, and particle size ≤38 μm). The mixtures were left with shaking for 2 h in water bath at 25°C, and then absorbance was measured. According to the results of preliminary adsorption experiments, the optimum calcination temperature was found as 800°C and applied throughout all adsorption experiments with equilibrium contact time 2 h.

The investigations on the impact of contact time were carried out at a temperature of 25°C. All other conditions remained unchanged (e.g., pH = 8, particle size ≤38 μm, and so on). The concentration of phosphate was

Table 1
Physical properties of JBA and CJBA

Physical properties	Bentonite	Calcinated bentonite
Bulk density	1.039 g/mL	1.034 g/mL
Porosity	60.7%	61.4%
SSA	438 m^2/kg	
CEC	138 mg/g	

Table 2
Approximate percentages of the bentonite (obtained by XRD analysis)

Compound name	Chemical formula
Silica	SiO_2
Palygorskite	$Mg_5Si_8O_{20}(OH)_2·8H_2O$
Hydrated halloysite	$Al_2Si_2O_5(OH)_4·2H_2O$
Anorthite, sodium, ordered	$(Ca, Na)(Al, Si)_2·Si_2O_8$
Iwakiite	$MnFe_2O_4$
Illite, trioctahedral	$K_{0.5}(Al, Fe, Mg)_3(Si, Al)_4O_{10}(OH)_2$

Table 3
Chemical composition (wt.%) of bentonite and calcinated bentonite samples (obtained by XRF analysis)

Compounds %	Bentonite	Calcinated bentonite
Na_2O	2.22	2.22
MgO	3.05	3.42
Al_2O_3	15.07	15.62
SiO_2	56.35	57.58
K_2O	2.66	2.8
CaO	2.03	2.19
TiO_2	1.64	1.49
Fe_2O_3	8.17	8.67

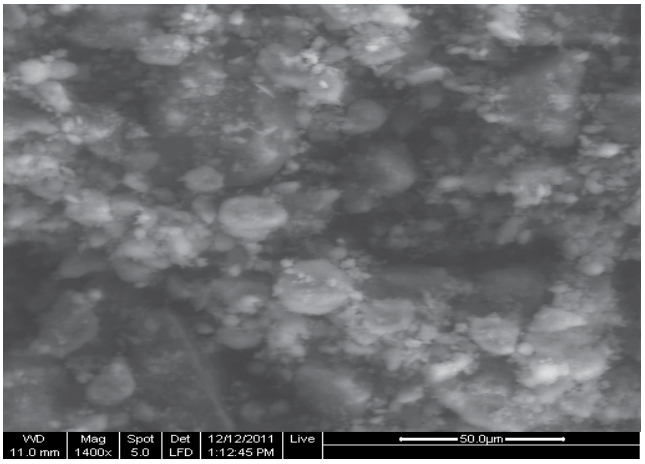

Fig. 1. Scanning electron micrograph of bentonite.

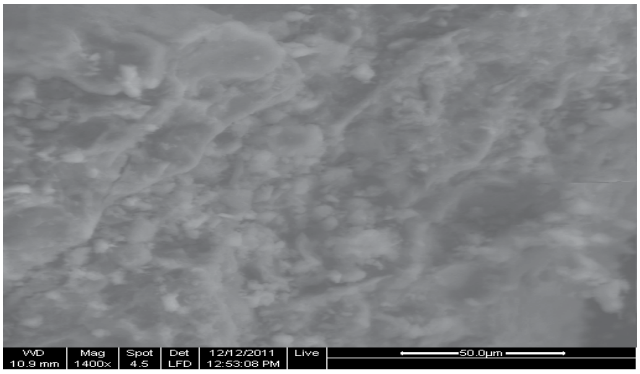

Fig. 2. Scanning electron micrograph of calcinated bentonite.

determined after 5, 10, 15, 30, 60 min, 1, 2, 4, 8, and 24 h, and then absorbance was measured. For the other studies, the equilibrium contact time was discovered to be 2 h.

Several studies were conducted to investigate the influence of temperature in the range (25°C, 35°C, 45°C, 55°C, and 65°C), (particle size ≤38 μm) (pH: 8). The following fraction of calcined bentonite particle size was used: ≤38, 38–63, 63–75, 75–90, 90–125, and 125 μm to study the effect of particle size while keeping the other experimental conditions constant.

The impact of pH ranging from 2 to 10 was also examined. The pH values were adjusted using NaOH and HCl, and the tests were carried out at a temperature of 25°C (particle size ≤38 μm).

Many experiments were carried out with starting concentrations ranging from 10–100 ppm while the other parameters remained constant (i.e., temperature at 25°C, pH equal 8, and particle size ≤ 38 m). The adsorbent dose in the range 0.5–2.5 g experiments were done also while keeping the other conditions constant.

For greater precision, all measurements were performed in duplicate, and the data was reported as the average of two values. The experimental error was found to be within 2.5%.

The specific amount of phosphate adsorbed was calculated from:

$$q_e = \frac{(C_o - C_e)V}{W} \tag{7}$$

where q_e is the adsorption capacity (mg/g) in the solid at equilibrium; C_o, C_e are initial and equilibrium concentrations of phosphate (mg/L), respectively; V is volume of the aqueous solution and W is the mass (g) of adsorbent used in the experiments [15].

2.3. Kinetic adsorption experiments

A 1,000 mL solution of phosphate ions (10 mg/L) was prepared, and then 5.0000 g of adsorbent was added and mixed in the reactor vessel for 24 h, the mixture was agitated with a mechanical stirrer at 1,000 rpm at a regulated temperature.

The kinetics of adsorption was carried out at various predetermined time durations throughout the 24 h by withdrawing the required aliquot from the reactor vessel, after centrifugation, the samples were analyzed. This investigation was done for different average particle sizes ≤38, 38–63, 63–75, 75–90, 90–125 and <125 μm, different pH with range of 6–9, different five temperatures 25°C, 35°C, 45°C, 55°C and 65°C and different three speed stirrer (agitation) 1,000; 2,000 and 3,000 rpm. The optimum calcination temperature 800°C was applied throughout all kinetics experiments. The kinetic studies were applied using synthetic and real wastewater samples.

All the concentrations of phosphate at different time intervals were determined in laboratory with colorimetric method using the indicator solution.

3. Results and discussion

3.1. Physical properties of bentonite

Porosity, bulk density, specific surface area, and CEC result are shown in Table 1, the results show that bentonite has high CEC this can explain the high performance of bentonite for removing phosphate form aqueous media. Bentonite minerals, silicates and oxides such as Al_2O_3 are effective for sorption [11].

The porosity and specific surface area (SSA) as shown in table, the large SSA explains the removal of phosphate from aqueous solution. Also the porosity is almost high (0.6) according to the range of porosity values for clay (0.4–0.7) [16]. This explains the efficiency of bentonite for phosphate removal.

3.2. XRF, XRD and SEM

The results of the current investigation are shown in Tables 2 and 3 for XRF and XRD. According to the XRF analysis, the percent composition of SiO_2 is 56.35 and 57.58 for bentonite and calcinated bentonite, respectively, and the percent composition of Al_2O_3 is 15.07 and 15.62 for bentonite and calcinated bentonite, respectively. The quantity of SiO_2 and Al_2O_3 increased after calcination, possibly due to partial breakdown of the octahedral layer, the SiO_2/Al_2O_3 ratios are 3.74 for bentonite and 3.67 for calcinated bentonite, which are more than one for both adsorbents. The ratio of Na_2O to CaO for bentonite and calcined bentonite

was 1.09 and 1.013, respectively, A value larger than one implies that the bentonite has excellent swelling [17]. XRD analysis reveals that bentonite minerals, silicates, and oxides such as Al_2O_3 and Fe_2O_3 are effective for sorption. The SEM picture (Fig. 1) illustrates that the bentonite sample has a large number of layers and sheets, which allow water to diffuse through them, then ion exchange, occur. SEM picture (Fig. 2) also shows that the surface area of the samples is larger, this means that the sorption will be very easy and very fast [12].

3.3. Batch studies

3.3.1. Effect of calcinations

The results in Fig. 3A show that increasing the temperature of calcinations in the range of 100°C–900°C may cause a decrease in the amount of hydroxyl (–OH) in bentonite. Since phosphate has a negative charge similar to hydroxyl, repulsion will take place, and as the porosity increases the efficiency of bentonite for removing phosphate increases. Additionally, calcinations will eliminate any impurities that may be present in the bentonite channels and that leading to increase the efficiency of removal as a result [13]. At 900°C, the efficacy of removal dropped, and collapsed action may have been taken place. 800°C was the ideal applied temperature used in the study of removing phosphate ions.

3.3.2. Effect of content time

The effect of contact time on the effectiveness of calcinated bentonite's capacity to extract phosphate was investigated (Fig. 3B). This adsorbent showed no significant increase in phosphate removal after reaching equilibrium in 2 h, as it becomes nearly impossible for additional phosphate molecules to diffuse deeper into the adsorbent structure at the highest energy sites due to phosphate aggregation and accumulation on the bentonite surface by increasing time [2,18]. Therefore, the appropriate equilibrium contact duration for future adsorption studies was determined to be 2 h.

3.3.3. Effect of initial concentration

The impact of the initial concentration of phosphate over the range from 10 to 100 mg/L on adsorption while keeping all other variables constant was investigated, the effectiveness and equilibrium absorption were evaluated at pH 8. It was found that the amount of phosphate adsorbed per gram of adsorbent at equilibrium increases by increasing initial concentration, which may be explained by an increase in the number of collisions between the reactants that lead to the observed ionization. This effect is seen in Fig. 3C, furthermore, due to the heterogeneous nature of the adsorbents' binding site distribution, it is projected that not all active sites would be equally effective [4].

3.3.4. Effect of pH

We measured how much phosphate was removed by calcined bentonite as a function of pH, as shown in Fig. 3D. Phosphate removal is reduced at acidic pH, which may be primarily due to the conversion of phosphate to phosphoric acid (H_3PO_4). Phosphate (H_3PO_4) is the most abundant species below pH 3.0 and binds weakly to adsorption sites. In this research, it was found that the maximum effective removal of phosphate ions by calcinated bentonite occurred in the pH range of 3–9. These results were explained by the presence of dominant dihydrogen and hydrogen phosphate $H_2PO_4^-$ and HPO_4^{2-} [19,20], Phosphate removal efficiency increased with increasing abundance of $H_2PO_4^-$ ions, suggesting that $H_2PO_4^-$ may have increased affinity for the adsorbent compared to H_3PO_4. Fig. 3D shows that the maximum efficiency of removal is in the pH range 7.0–9.0. The monovalent ion, $H_2PO_4^-$, is known to predominate in solutions at pH values at pH values between 3 and 6 and may have a higher affinity for solid sorbents compared to the forms present at other pH values whereas at higher pH values, the divalent anion HPO_4^{2-} dominates ($pK_{a1} = 2.23$, $pK_{a2} = 7.21$, $pK_{a3} = 12.32$).

At pH 10, more hydroxyl ions may compete for active adsorption sites and increases of the negative charge on the adsorbent surface will take place, the concentration of HPO_4^{2-} ion increases resulting in higher electrostatic repulsion. HPO_4^{2-} which may be responsible for the decreased phosphate uptake [21].

3.3.5. Effect of adsorbent dosage

One of the most significant factors in the removal process is adsorbent dosage, which is the ratio of the mass of adsorbent to the volume of solution. The effect of sorbent dose on the phosphate removal of calcinated bentonite was studied in the range of 0.5–2.5 g and the results are shown in Fig. 3E. It was observed that the cumulative removal rate of phosphate ions increased with increasing calcinated bentonite dose (from 34.97% to 90.94%) this may be attributed to the increased total area and the sites of adsorption will be more. On the other hand, the mass uptake per unit of adsorbent (q, mg/g) decreased with increasing dose of calcinated bentonite (from 0.325 to 0.0091 mg/g), this may be related to the abundance of adsorption sites [22].

3.3.6. Effect of temperature

Fig. 3F illustrates the influence of temperature on phosphate removal using calcinated bentonite while all other parameters were held constant; under five various temperatures values 25°C, 35°C, 45°C, 55°C, and 65°C. It was found that increasing the temperature increased the percentage of phosphate removal, indicating that the process is endothermic. Between 55°C and 65°C, the uptake is nearly constant. These findings might be explained by the availability of additional adsorbent active sites, and/or adsorbent surface will be activated at higher temperatures and might possibly be attributed to enhanced phosphate ion mobility from the bulk solution to the adsorbent surface, which boosted penetration inside calcinated bentonite [23].

3.3.7. Effect of particle size

The effect of particle size on phosphate adsorption was investigated with six different particle sizes ranging from (≤38–≥125) μm. As shown in Fig. 3H, the phosphate removal

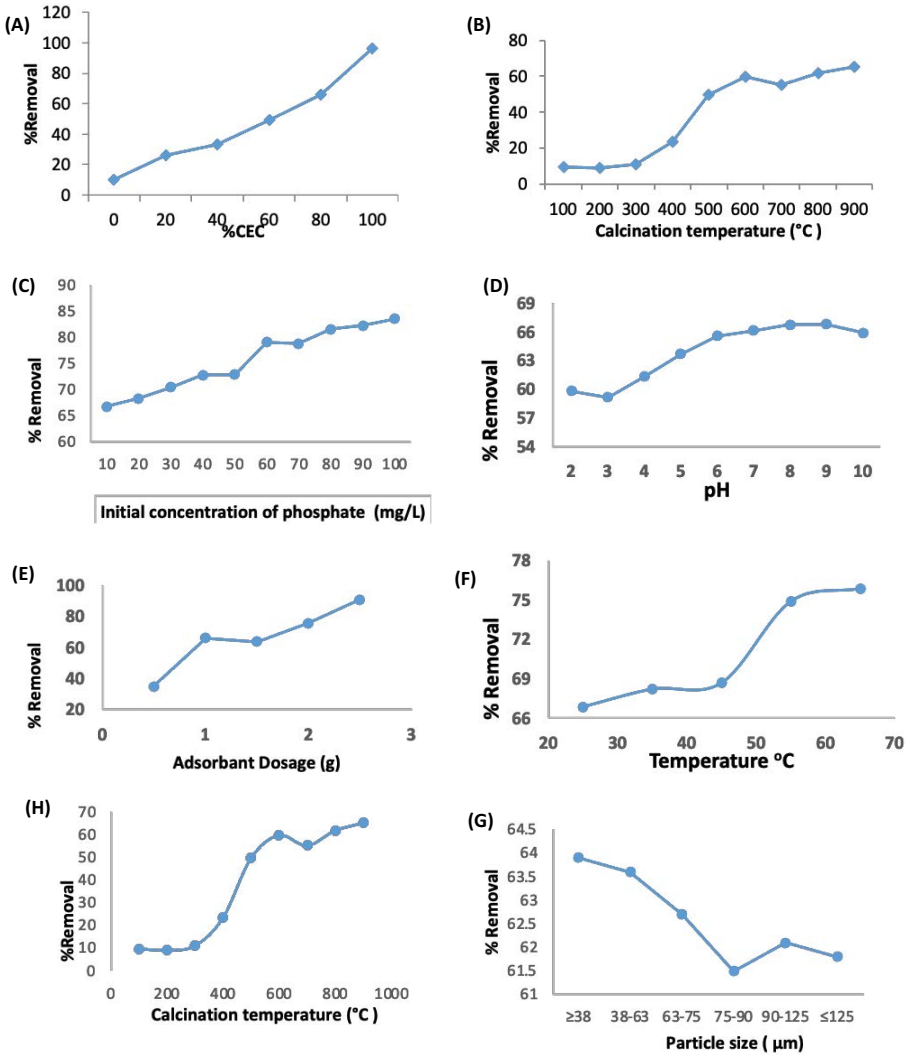

Fig. 3. Effect of different variables on the removal of PO_4^{-3} onto using calcinated bentonite. (A) %CEC, (B) calcination temperature, (C) initial concentration, (D) pH, (E) adsorbent dosage, (F) temperature, (G) contact time and (H) particle size.

rate increased with decreasing particle size and the entrapment efficiency ranged (63.9%–61.8%). This is because adsorption is a surface area phenomenon, and the smaller the size of the adsorbent, the larger the surface area [1].

4. Kinetic studies

4.1. Kinetic studies for synthetic phosphate solution

To investigate the reaction order of an ion exchange process, the phosphate sorption constants were calculated using Eqs. (1) and (2) for pseudo-first and second-order rate models. Linear regression was frequently used to determine the best fitted model, and the method of least squares was frequently used to find the parameters of these models. The pseudo-first and pseudo-second-order rate constants, correlation coefficients, and equilibrium sorption capacities of phosphate ions under different conditions were calculated, as shown in Table 4, R^2 values for the pseudo-second-order kinetic equal (0.99–1) at various variables (temperature, pH, particle size, and agitation speed) are actually greater than those for the pseudo-first-order model, confirming that the kinetics of phosphate sorption onto calcinated bentonite follows the pseudo-second-order rate expression.

It was discovered that increasing the temperature increased the equilibrium removal capacity of phosphate ion, q_{e2}, which indicates a high temperature favor, which might be due to a tendency for the phosphate ion to escape from the bulk phase to the solid phase and an increase in the driving force. Because sorption is an endothermic process, an increase in solution temperature should result in an increase in sorption capacity [11,12].

Table 4 shows that increasing the pH values causes a slight decrease in k_2 values. This could be due to an increase in the negative charge on the surface of the solid sorbent, which causes repulsion between the solid surface and the ions [20]. The data in Table 4 show that the rate (k_2) of phosphate ion uptake increased as the mean diameter of the calcinated bentonite decreased, owing to the increase in surface area, but q_{e2} increased as particle size decreased.

Table 4
Kinetic study (synthetic phosphate solution) for calcinated bentonite. The effect of temperature, pH, particle size and agitation speed. C_o = 10 ppm and the solid bentonite concentration is 5 g/995 mL

Temperature (°C)	Second-order					First-order				Intraparticle diffusion	
	$q_{e,exp}$	$q_{e,2nd}$	% SD	k_2	R^2	$q_{e,1st}$	% SD	k_1	R^2	D_p (m²/s)	D_f (m²/s)
25	0.159	0.162	0.493	0.155	0.999	0.111	9.574	1.610×10^{-3}	0.884	2.430×10^{-13}	4.150×10^{-15}
35	0.170	0.173	0.533	0.169	0.999	0.069	19.518	1.640×10^{-3}	0.931	2.710×10^{-13}	4.940×10^{-15}
45	0.172	0.176	0.704	0.168	0.999	0.117	10.106	1.370×10^{-3}	0.935	2.200×10^{-13}	4.360×10^{-15}
55	0.175	0.180	0.865	0.228	0.999	0.123	9.361	2.000×10^{-3}	0.753	1.140×10^{-13}	2.080×10^{-15}
65	0.178	0.183	0.851	0.227	0.999	0.121	10.121	1.420×10^{-3}	0.951	2.800×10^{-13}	5.390×10^{-15}
pH											
6	0.137	0.139	0.441	0.278	0.999	0.078	13.828	1.280×10^{-3}	0.929	2.170×10^{-13}	3.180×10^{-15}
7	0.147	0.150	0.575	0.297	0.999	0.083	14.015	1.470×10^{-3}	0.920	8.830×10^{-14}	1.330×10^{-15}
8	0.159	0.162	0.493	0.227	0.999	0.111	9.574	1.420×10^{-3}	0.951	2.430×10^{-13}	4.150×10^{-15}
9	0.169	0.171	0.357	0.220	0.999	0.093	14.478	1.000×10^{-3}	0.930	1.670×10^{-13}	3.150×10^{-15}
Particle size											
≤38 μm	0.159	0.162	0.493	0.277	0.999	0.111	9.574	1.420×10^{-3}	0.951	2.430×10^{-13}	4.150×10^{-15}
38–63 μm	0.148	0.151	0.613	0.245	0.999	0.096	11.155	1.800×10^{-3}	0.893	4.470×10^{-13}	5.520×10^{-15}
63–75 μm	0.146	0.150	0.788	0.2529	0.999	0.095	11.087	1.910×10^{-3}	0.890	2.450×10^{-13}	4.190×10^{-15}
75–90 μm	0.146	0.148	0.519	0.288	0.999	0.094	11.242	2.000×10^{-3}	0.934	5.260×10^{-13}	3.570×10^{-15}
90–125 μm	0.145	0.149	0.708	0.256	0.999	0.078	14.941	1.730×10^{-3}	0.855	2.540×10^{-12}	1.260×10^{-14}
≥125 μm	0.145	0.148	0.583	0.261	0.999	0.087	12.816	1.910×10^{-3}	0.811	4.620×10^{-12}	2.080×10^{-14}
Agitation (rpm)											
1,000	0.159	0.162	0.493	0.227	0.999	0.111	9.574	1.420×10^{-3}	0.951	2.430×10^{-13}	4.150×10^{-15}
2,000	0.170	0.173	0.552	0.224	0.999	0.092	14.780	1.570×10^{-3}	0.867	2.730×10^{-13}	4.930×10^{-15}
3,000	0.170	0.174	0.712	0.248	0.999	0.103	12.577	1.360×10^{-3}	0.934	2.290×10^{-13}	4.260×10^{-15}

Table 4 also shows that increasing the agitation increases k_2 because phosphate ions face resistance at the liquid phase, via the boundary layer, on their way to the solid phase The agitation of suspensions during experiments reduced the boundary layer and the resistance to phosphate ion transport. This increases the ion transfer rate and adsorption [24].

Ion exchange kinetics were studied using diffusion models. The kinetics data experiments were used to fit both the film and particle diffusion models. As shown in Table 4, Vermilion's particle diffusion model approximation provided better correlation for all samples at different variables. The fact that the film diffusion coefficients in the ion exchanger are lower than the particle diffusion coefficients confirms that the film diffusion coefficients control the rate of phosphate ion uptake [11].

4.2. Kinetic studies for wastewater

In wastewater kinetic studies, we will see a significant difference in the efficiency of phosphate removal between synthetic and real wastewater samples. The removal rate difference between synthetic phosphate solution and wastewater nearly doubled for synthetic phosphate solution. This is due to the presence of impurities in wastewater. According to the data in Table 5, real wastewater behaves almost identically to synthetic wastewater, but its efficiency is lower.

The pseudo-first and pseudo-second-order rate constants, correlation coefficients, and equilibrium sorption capacities of phosphate ions under various conditions were calculated, as shown in Table 5. R^2 values for the pseudo-second-order kinetic, which are less than that of the synthetic sample at various variables (temperature, pH, particle size, and agitation speed), are actually greater than those for the pseudo-first-order model, proving that the pseudo-second-order rate expression is followed by the kinetics of phosphate sorption onto calcinated bentonite.

The information in Table 5 demonstrates that as the mean diameter of the calcinated bentonite expanded, the rate (k_2) of phosphate ion uptake increased. This may be due to interference from impurities, while q_{e2} reduced as particle size increased. Table 5 also demonstrates that decreasing k_2 occurs with increasing agitation; this may be due to competition between the phosphate ions and other foreign ions in the solid phase. It is also confirmed that the film diffusion coefficients regulate the rate of phosphate ion uptake since they are lower than the particle diffusion coefficients [11].

4.3. Activation energy

the activation energy was determined using the Arrhenius equation, which is:

Table 5
Kinetic study (wastewater) for calcinated bentonite. The effect of temperature, pH, particle size and agitation speed. C_o = 10ppm and the solid bentonite concentration is 5 g/995 mL

Temperature (°C)	Second-order					First-order				Intraparticle diffusion	
	$q_{e,exp}$	$q_{e,2nd}$	% SD	k_2	R^2	$q_{e,1st}$	% SD	k_1	R^2	D_p (m²/s)	D_f (m²/s)
25	0.07	0.0696	19.219	0.212	0.998	0.038	74.697	9.980×10^{-4}	0.950	6.870×10^{-14}	6.740×10^{-16}
35	0.076	0.076	2.816	0.211	0.995	0.048	14.061	8.805×10^{-4}	0.930	6.740×10^{-14}	7.700×10^{-16}
45	0.083	0.083	13.114	0.240	0.992	0.050	48.564	6.030×10^{-4}	0.906	9.570×10^{-14}	1.040×10^{-15}
55	0.098	0.099	7.987	0.230	0.999	0.060	36.670	4.680×10^{-4}	0.960	1.450×10^{-13}	1.820×10^{-15}
65	0.117	0.119	1.036	0.320	0.994	0.013	564.203	4.640×10^{-4}	0.82	1.63×10^{-13}	2.500×10^{-15}
pH											
6	0.0851	0.049	2.547	0.350	0.98	0.024	90.851	1.730×10^{-4}	0.670	2.450×10^{-14}	1.800×10^{-16}
7	0.064	0.063	9.352	0.330	0.99	0.033	56.118	3.300×10^{-4}	0.777	4.750×10^{-14}	4.360×10^{-16}
8	0.07	0.0696	19.219	0.320	0.994	0.038	74.697	4.640×10^{-4}	0.820	6.870×10^{-14}	6.740×10^{-16}
9	0.077	0.077	6.461	0.310	0.997	0.043	41.205	5.470×10^{-4}	0.940	8.370×10^{-14}	8.760×10^{-16}
Particle size											
≤38 μm	0.07	0.0696	19.219	0.320	0.994	0.038	74.697	4.640×10^{-4}	0.820	6.870×10^{-14}	6.740×10^{-16}
38–63 μm	0.072	0.072	10.555	0.338	0.998	0.043	44.068	6.730×10^{-4}	0.950	1.830×10^{-13}	1.330×10^{-15}
63–75 μm	0.067	0.067	13.394	0.390	0.998	0.039	52.666	6.990×10^{-4}	0.953	1.440×10^{-12}	3.520×10^{-15}
75–90 μm	0.063	0.063	15.937	0.370	0.996	0.035	63.743	3.000×10^{-4}	0.943	3.780×10^{-13}	1.500×10^{-15}
90–125 μm	0.054	0.054	14.298	0.450	0.997	0.031	56.161	6.640×10^{-4}	0.99	8.460×10^{-13}	2.080×10^{-15}
≥125 μm	0.051	0.051	23.548	0.400	0.994	0.036	51.837	6.000×10^{-4}	0.95	1.020×10^{-12}	2.050×10^{-15}
Agitation (rpm)											
1,000	0.07	0.0696	19.219	0.320	0.994	0.038	74.697	4.640×10^{-4}	0.82	6.870×10^{-14}	6.740×10^{-16}
2,000	0.084	0.084	2.913	0.230	0.991	0.051	27.177	5.940×10^{-4}	0.89	9.436×10^{-14}	1.058×10^{-15}
3,000	0.116	0.116	3.436	0.210	0.998	0.081	8.525	1.010×10^{-3}	0.96	1.660×10^{-13}	2.510×10^{-15}

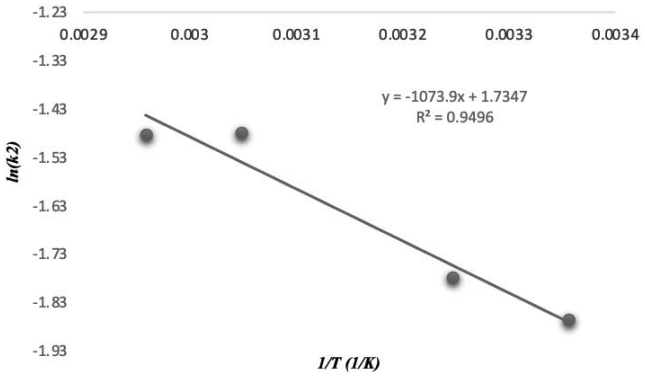

Fig. 4. Activation energy for the removal of PO_4^{-3} from synthetic aqueous solutions using calcinated bentonite.

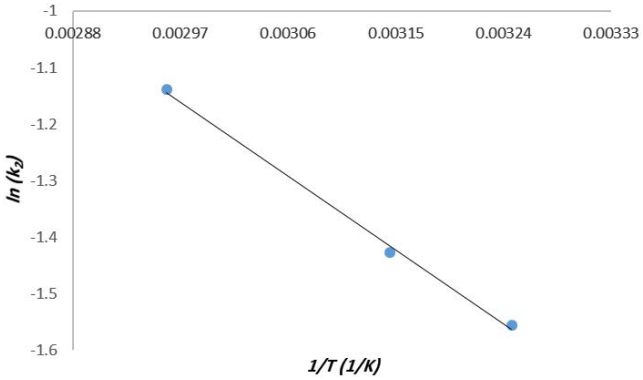

Fig. 5. Activation energy for the removal of PO_4^{-3} from real aqueous solutions using calcinated bentonite.

$$\ln k_2 = -\left(\frac{E_a}{RT}\right) + \ln A \quad (8)$$

where R is the gas constant, T is temperature (°K), A is the Arrhenius factor, E_a is the activation energy in kJ/mol, and k_2 is the second-rate constant for removal in g/mg·s. The activation energy was determined by plotting $\ln(k_2)$ vs. $1/T$; based on the slope of this plot, the E_a were calculated, and the removal activation energies for both synthetic and actual samples were determined to be 8.93 and 12.120 kJ/mol, respectively as shown in Figs. 4 and 5 which means physisorption may take place. If the activation energy is between 5 and 40 kJ/mol, the process is physisorption; however, if it is between 40 and 800 kJ/mol, which is higher than physisorption, the process is chemisorption [11,14].

4.3.1. Validation test

The sum of error squares (SSE%) is determined using Eq. (9) to assess the reliability and applicability of the pseudo-second-order kinetic model [11]:

$$\Delta q = \text{S.D} = \sqrt{\frac{\sum\left[\frac{\left(q_{e,\exp} - q_{e,\text{cal}}\right)}{q_{e,\exp}}\right]^2}{n-1}} \quad (9)$$

The calculated $q_{e,\text{cal}}$ were found close the experimental $q_{e,\exp}$ using the synthetic waste water at all temperatures as shown Table 4, these results indicate that this model fits well to describe the adsorption kinetics, while Table 5 for the real waste water showed that the calculated values of $q_{e,\text{cal}}$ were not close the experimental $q_{e,\exp}$, may be of the impurities

5. Conclusion

The percent of removal of phosphate ion by was investigated using Jordanian calcinated bentonite by applying the batch experiments of the removal of synthetic and real samples of phosphate ions in aqueous media at different variables, (calcinations, initial concentration of phosphate ions, temperature particle size, pH values, adsorbent dosage and contact time) specific conclusions based on the findings of this study was screened.

The results showed that the percent of removal increased by increasing the calcination temperature (100°C–900°C), the percent of removal increased by increasing the initial concentration of phosphate ions, the percent of removal increased by increasing the pH values and the agitation speed. The percent of removal was decreased by increasing particle size. The effect of temperature was studied in the range of 25°C–65°C the percent of removal was increased by increasing the temperature which indicate the process is an endothermic one. The effect of contact time shows that at first 5 min the percent was very high, then go slowly until reach to equilibrium within 2 h and the percent of removal was increased by increasing the adsorbent dosage. Kinetic studies were investigated for synthetic and real wastewater using pseudo-second-order and diffusion models, the R^2 values showed that the pseudo-second-order equation was the most appropriate model for the description of phosphate transport. Both particle diffusion (D_p) and film diffusion (D_f) coefficients were found at different variables like (temperature, particle size, agitation, pH values). These results were obtained for synthetic phosphate solution and real wastewater, result indicated that the rate determine step is film diffusion (D_f). The calculated activation energy proves that the process is physisorption one.

Acknowledgement

The authors are grateful to the financial support from the Deanship of graduate studies of Al Al-Bayt University.

References

[1] Y. Fetene, T. Addis, Adsorptive removal of phosphate from wastewater using Ethiopian rift pumice: batch experiment, Air Soil Water Res., 13 (2020) 1–12.
[2] N.A.A. Aboud, B.E. Jasim, A.M. Rheim, Adsorption study of phosphate ions pollution in aqueous solutions using microwave synthesized magnesium oxide nanoparticles, Dig. J. Nanomater. Biostruct., 16 (2021) 801–807.
[3] B. Wu, J. Wan, Y. Zhang, B. Pan, I.M.C. Lo, Selective phosphate removal from water and wastewater using sorption: process fundamentals and removal mechanisms, Environ. Sci. Technol., 54 (2020) 50–66.
[4] D.T. Mekonnen, E. Alemayehu, B. Lennartz, Removal of phosphate ions from aqueous solutions by adsorption onto leftover coal, Water, 12 (1381) 1–15.
[5] T. Clark, T. Stephenson, P.A. Pearce, Phosphorus removal by chemical precipitation in a biological aerated filter, Water Res., 31 (1997) 2557–2563.
[6] P. Xia, X. Wang, X. Wang, J. Song, H. Wang, J. Zhang, J. Zhao, Struvite crystallization combined adsorption of phosphate and ammonium from aqueous solutions by mesoporous MgO-loaded diatomite, Colloids Surf., A, 506 (2016) 220–227.
[7] C. Pratt, S.A. Parsons, A. Soares, B.D. Martin, Biologically and chemically mediated adsorption and precipitation of phosphorus from wastewater, Curr. Opin. Biotechnol., 23 (2012) 890–896.
[8] M.O. Usman, G. Aturagaba, M. Ntale, G.W. Nyakairu, A review of adsorption techniques for removal of phosphates from wastewater, Water Sci. Technol., 86 (2022) 3113–3132.
[9] K. Nobaharan, S.B. Novair, B.A. Lajayer, E.D. van Hullebusch, Phosphorus removal from wastewater: the potential use of biochar and the key controlling factors, Water, 13 (2021) 1–20.
[10] A. Hossam Elgarhy, B.N.A. Mahran, G. Liu, T.A. Salem, E.E. ElSayed, L.A. Ibrahim, Comparative study for removal of phosphorus from aqueous solution by natural and activated bentonite, Sci. Rep., 12 (2022) 19433, doi: 10.1038/s41598-022-23178-w.
[11] H.M. Baker, Removal of lead ions from wastewater using modified Jordanian zeolite, Chem. Sci. Int. J., 29 (2020) 19–30.
[12] H.M. Baker, A.M. Massadeh, H.A. Younes, Natural Jordanian zeolite: removal of heavy metal ions from water samples using column and batch methods, Environ. Monit. Assess., 157 (2009) 319–330.
[13] M.G.A. Vieira, A.F. Almeida Neto, M.L. Gimenes, M.G.C. da Silva, Sorption kinetics and equilibrium for the removal of nickel ions from aqueous phase on calcined Bofe bentonite clay, J. Hazard. Mater., 177 (2010) 362–371.
[14] H.M. Baker, H. Fraij, Principles of interaction of ammonium ion with natural Jordanian deposits: analysis of uptake studies, Desalination, 251 (2010) 41–46.
[15] Y. Amano, M. Machida, T. Sakamoto, Phosphate ion adsorption properties of PAN-based activated carbon fibers prepared with K_2CO_3 activation, SN Appl. Sci., 2 (2020) 1–8.
[16] C. Yu, C. Loureiro, J.-J. Cheng, L.G. Jones, Y.Y. Wang, Y.P. Chia, E. Faillace, Data Collection Handbook to Support Modeling the Impacts of Radioactive Material in Soil, Environmental Assessment and Information Sciences Division, Argonne National Laboratory, 9700 South Cass Avenue, Argonne, Illinois 60439, April 1993.
[17] M.A. Usman, V.I. Ekwueme, T.O. Alaje, A.O. Mohammed, Characterization, acid activation, and bleaching performance of Ibeshe clay, Lagos, Nigeria, Int. Sch. Res. Notices, 2012 (2012) 658508, doi: 10.5402/2012/658508.
[18] P.R. Rout, P. Bhunia, R. Roshan Dash, A mechanistic approach to evaluate the effectiveness of red soil as a natural adsorbent for phosphate removal from wastewater, Desal. Water Treat., 54 (2014) 358–373.
[19] W. Chouyyok, R.J. Wiacek, K. Pattamakomsan, T. Sangvanich, R.M. Grudzien, G E. Fryxell, Phosphate removal by anion binding on functionalized nanoporous sorbents, Environ. Sci. Technol., 44 (2010) 3073–3078.

[20] X. Xu, B. Wang, H. Tang, Z. Jin, T. Huang, Removal of phosphate from wastewater by modified bentonite entrapped in Ca-alginate beads, J. Environ. Manage., 260 (2020) 1–7.
[21] P. Paul, S. Parbat, G. Aditya, Phosphate ion removal from aqueous solution using snail shell dust: biosorption potential of waste shells of edible snails, RSC Adv., 12 (2022) 30011–30023.
[22] A. Abdelhay, A. Al Bsoul, A. Al-Othman, N.M. Al-Ananzeh, I. Jum'h, A.A. Al-Taani, Kinetic and thermodynamic study of phosphate removal from water by adsorption onto (*Arundo donax*) reeds, Adsorpt. Sci. Technol., 36 (2017) 1–16, doi: 10.1177/026361741668437.
[23] Y. Shu, L. Li, Q. Zhang, H. Wu, Equilibrium, kinetics and thermodynamic studies for sorption of chlorobenzenes on CTMAB modified bentonite and kaolinite, J. Hazard. Mater., 173 (2010) 47–53.
[24] S.J. Kang, K. Wada, An assessment of the effectiveness of natural zeolites for removal of ammonium and zinc from their dilute solutions, Appl. Clay Sci., 3 (1988) 281–290.